Electronic Supplementary Material (ESI) for Physical Chemistry Chemical Physics.
This journal is © the Owner Societies 2017

Supplementary Information

A fluorescence-electrochemical study of carbon nanodots (CNDs) in bio- and photoelectronic application and energy gap investigation

*Zheng Zeng,[1#] Wendi Zhang,[1#] Durga Manjari Arvapalli,[1] Brian Bloom,[2] Alex Sheardy,[1] Taylor Mabe,[1] Yiyang Liu,[1] Zuowei Ji,[1] Harish Chevva,[1]David H. Waldeck,[2] Jianjun Wei[1]**

[1]Department of Nanoscience, Joint School of Nanoscience and Nanoengineering, University of North Carolina at Greensboro, Greensboro, NC 27401, USA.

[2]Department of Chemistry, University of Pittsburgh, Pittsburgh, PA 15260, USA.

[#] Equal contribution

AUTHOR INFORMATION

Corresponding Author

* j_wei@uncg.edu

Characterization

AFM Image and profile:

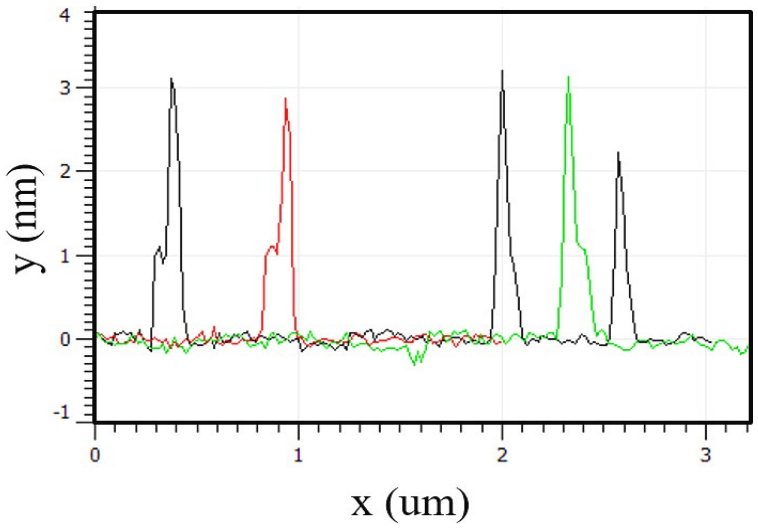

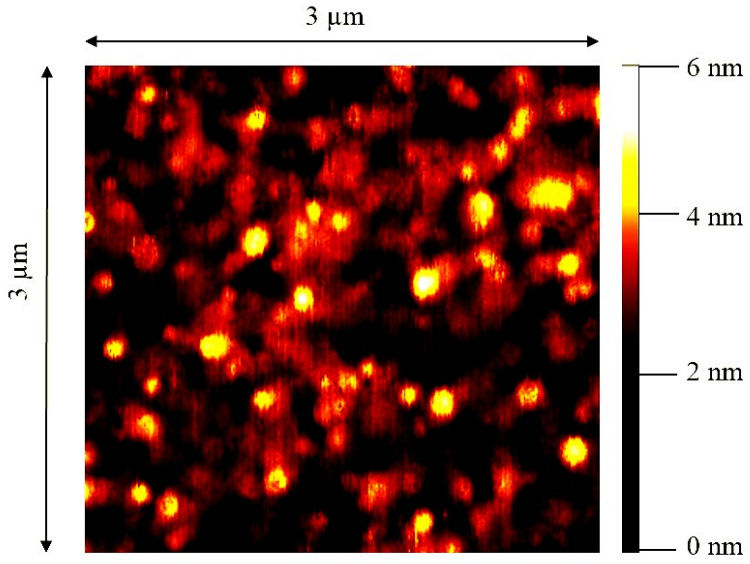

Fig. S1. AFM cross section profile for Figure 1b and AFM analysis of the CNDs immobilized on the gold slide electrode surface.

XPS:

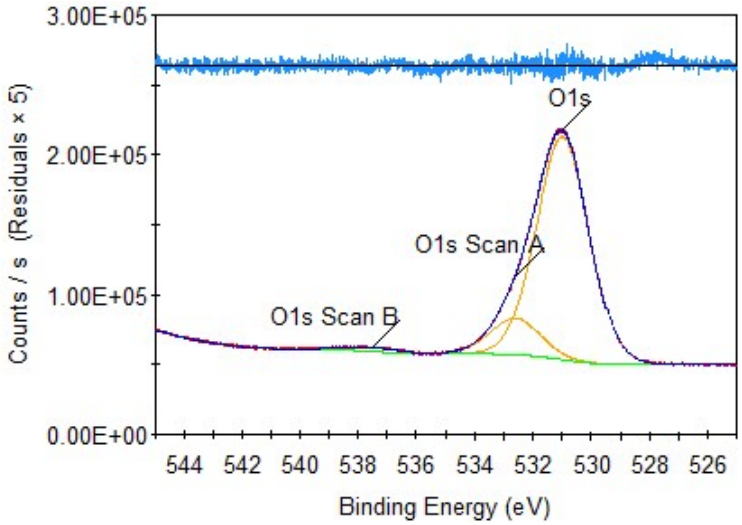

Fig. S2. High resolution O XPS spectrum and its simulated peak fit

Table S1. High resolution O XPS spectrum analysis

Name	Start BE	Peak BE	End BE	Height CPS	FWHM eV	Area (P) CPS.eV	Area (N) TPP-2M	Atomic %
O1s	544.99	530.95	525.01	159349.07	2.07	357909.21	0.86	84.81
O1s Scan A	544.99	532.59	525.01	26334.66	2.01	57238.62	0.14	13.57
O1s Scan B	544.99	537.53	525.01	3017.5	2.08	6788	0.02	1.61

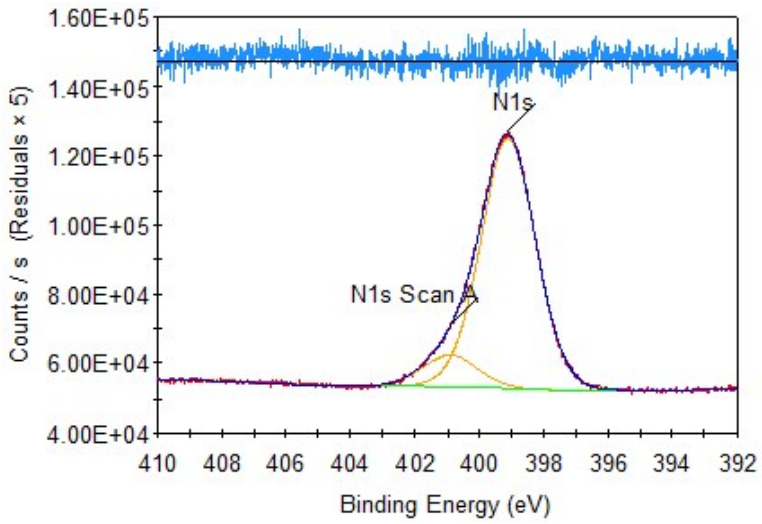

Fig. S3. High resolution N XPS spectrum and its simulated peak fit

Table S2. High resolution N XPS spectrum analysis

Name	Start BE	Peak BE	End BE	Height CPS	FWHM eV	Area (P) CPS.eV	Area (N) TPP-2M	Atomic %
N1s	409.99	399.11	392.01	72523.1	1.98	155646.87	0.61	88.8
N1s Scan A	409.99	400.9	392.01	9222.81	1.96	19610.83	0.08	11.2

Table S3. Survey XPS spectrum analysis

Name	Start BE	Peak BE	End BE	Height CPS	FWHM eV	Area (P) CPS.eV	Area (N) TPP-2M	Atomic %
O1s	541.5	531.65	523	315606.48	3.92	1336206.35	0.85	27.1116
N1s	406	399.8	394.5	133751.39	3.68	527094.38	0.53	17.0188
C1s	293	286.14	278	184033.28	5.79	1065537.72	1.7	54.3737

Zeta potential:

Table S4. Zeta potential measurement of CNDs

pH	Dispersion name	Dispersion refractive index	Temperature	Zeta runs	Zeta Potential
5.86	Water	1.330	25 ˚C	12	-22.3 mV

Quantum yield:

Table S5. Quantum yield measurement of CNDs

Sample	Refractive index(η)	Quantum yield(Q)
Quinine sulfate	1.33	0.54
CNDs	1.33	0.085

The quantum yield (Q) of as-prepared CNDs was investigated according to established methods[1]. Quinine sulfate (quantum yield 0.54 at 360 nm) dissolved in 0.1 M H_2SO_4 (refractive index(η_R)=1.33) was chosen as reference. As-prepared CNDs were dispersed in deionized water (η_x=1.33). All samples were tested to obtain absorption intensities by UV-Vis spectrometer (Varian Cary 6000i). In order to minimize re-absorption effects, the UV-Vis absorbance was kept under 0.1 OD, and the photoluminescence (PL) was measured at an excitation wavelength of 360 nm (Varian Cary Eclipse). The quantum yield was calculated based on the following equation:

$$Q_x = Q_R \times \frac{I_x}{I_R} \times \frac{A_R}{A_x} \times \frac{\eta_x^2}{\eta_R^2}$$

where Q is quantum yield, *I* is integrated PL intensity of the sample, A is the absorbance intensity, η is the refractive index for the solvent, X means as-prepared CNDs, and R refers to quinine sulfate as reference fluorophore.

Bioimaging

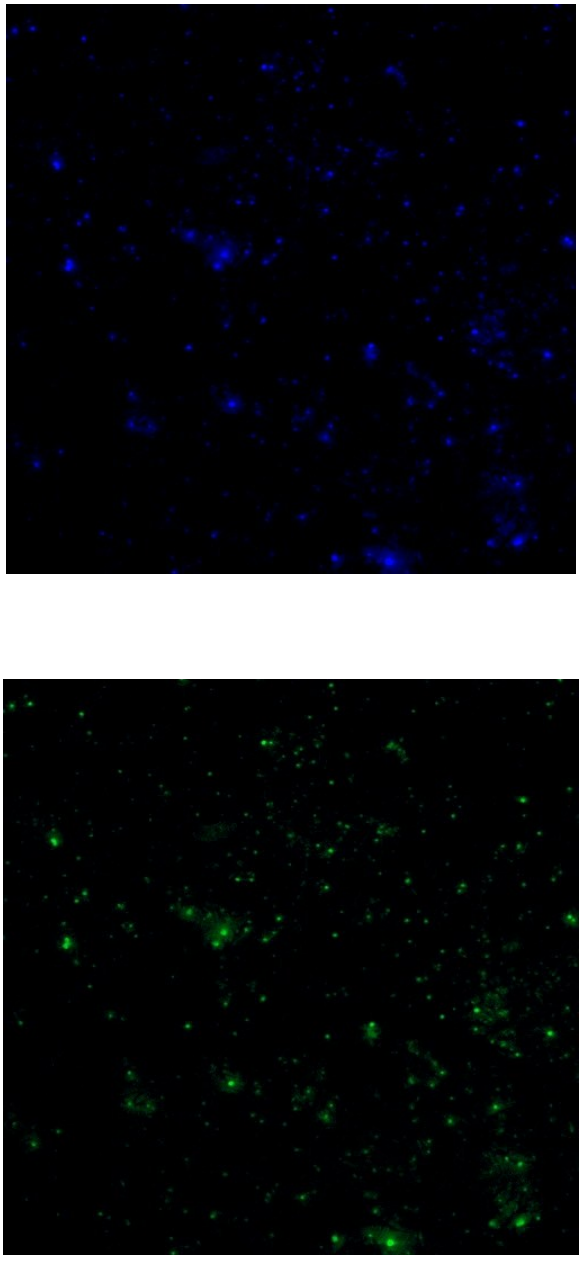

Fig. S4. Confocal images of HepG2 cells cultured treated with CNDs (0.3 mg/mL) for 72 hours.

Electrochemistry causes fluorescence of CNDs to change

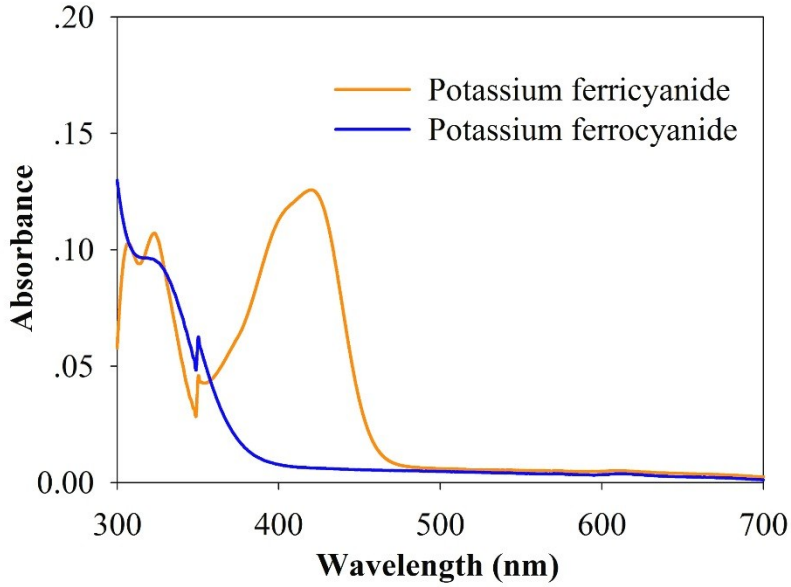

Fig. S5. UV-Vis absorption spectrum of CNDs potassium ferricyanide and potassium ferrocyanide.

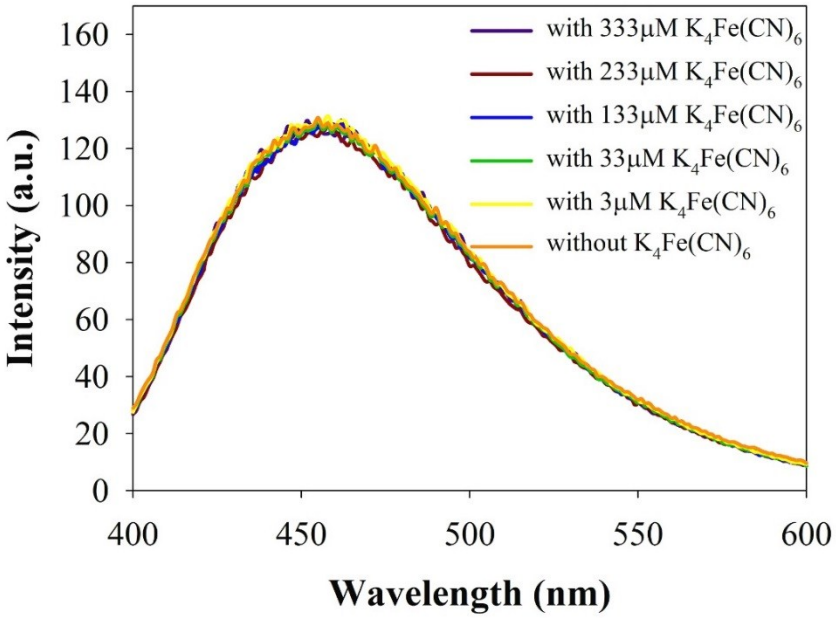

Fig. S6. Fluorescence spectrum of solution including 50 μg/mL CNDs and 0.1 M KCl after addition of $K_4Fe(CN)_6$ with different concentrations (3, 33, 133, 233, and 333 μM).

Light from the fluorescence spectrophotometer causes CNDs to generate photocurrent

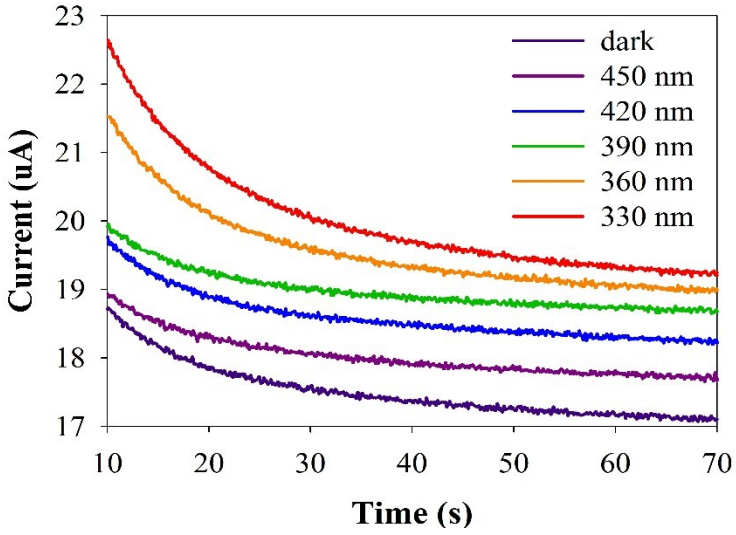

Fig. S7 Chronoamperometry (CA) measurements with an applied voltage of 0.8 V of the gold slide electrode with CNDs immobilization before and after light irradiation with different incident wavelength (330-450 nm).

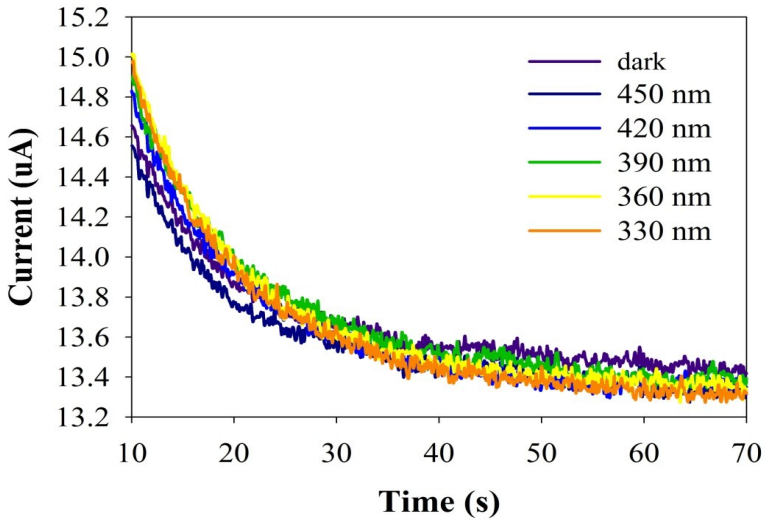

(a)

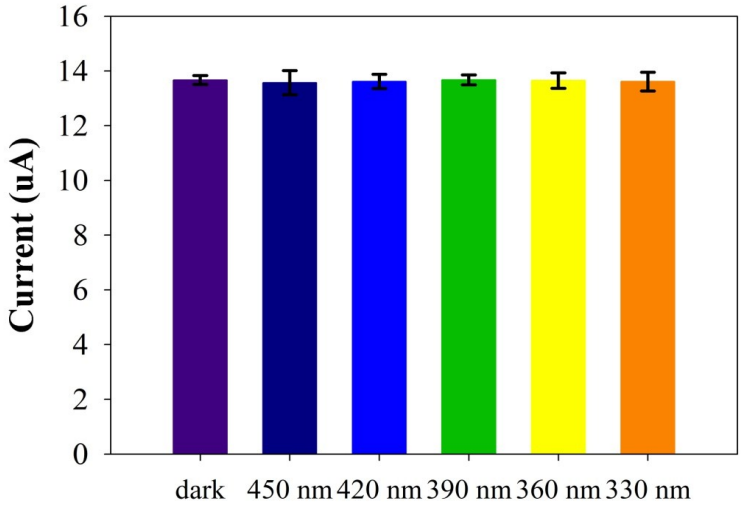

(b)

Fig. S8. Chronoamperometry (CA) measurements with an applied voltage of 0.8 V of the gold slide electrode without CNDs immobilization before and after light irradiation with different incident wavelength (330-450 nm).

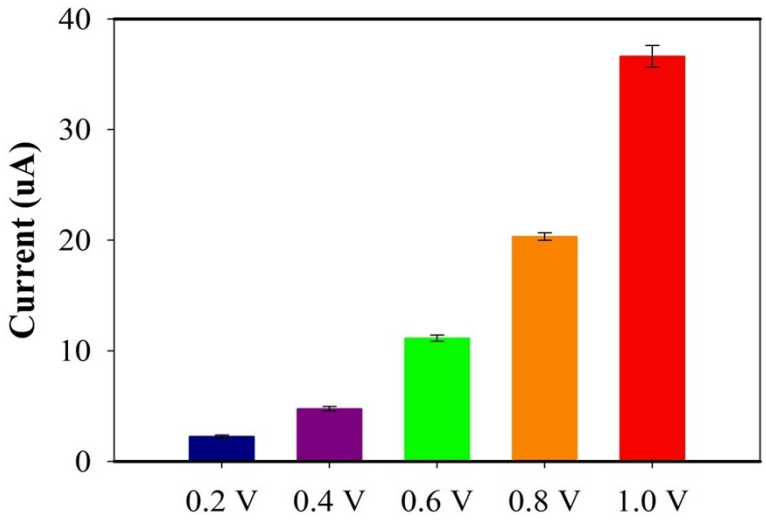

Fig. S9. CA measurement with different applied potentials of the gold slide electrode with CNDs immobization under incident wavelength of 330 nm.

Band energy and molecular orbital energy level

Method 1. Optical band gap and exciton binding energy calculation

Since coulomb and resonance integral values should be taken into account in the CNDs system, the indirect band gap formula in the semiconductor system was used:[2]

$\alpha h\nu=C(h\nu-E_o)^2$

where α is the absorption coefficient, h is the Plank constant, ν is the frequency, C is the coefficient, and E_o is the optical band gap, $(\alpha h\nu)^{1/2}$ has a linear relationship with hν, which could be used to estimate E_o. The Beer-Lambert law states that

$A=\alpha bc$,

where A is the measured absorbance, b is the path length, and c is the analyte concentration. Among them, b and c are fixed values, so the E_o could be calculated as the following equation:

$(Ah\nu/bc)^{1/2}=D(h\nu-E_o)$,

where $(Ah\nu/bc)^{1/2}$ has a linear relationship with hν with a slope of D and E_o is the x-intercept. Note that hν is equal to 1240/λ in units of eV. In addition, changing the path length and concentration did not affect the result of x-intercept (E_o). With the UV-Vis absorption spectrum results, the relationship $(Ah\nu)^{1/2}$ vs. hν could be used to estimate E_o as 2.13 eV.

Moreover, the exciton binding energy (E_b) can be estimated by the hydrogenic model:

$E_b = \mu R_H/m_0\varepsilon^2$,

where μ is the effective reduced mass of the exciton, R_H is the Rydberg constant of the hydrogen atom (13.6 eV), m_0 is the free electron mass, and ε is the dielectric constant. With the assumption of $\mu=0.1\ m_0$, depending on the value used for ε, estimated values for E_b range from 6.1 meV to 13.6 meV.[3,4]

Method 2. Electrochemical measurement energy gap calculation

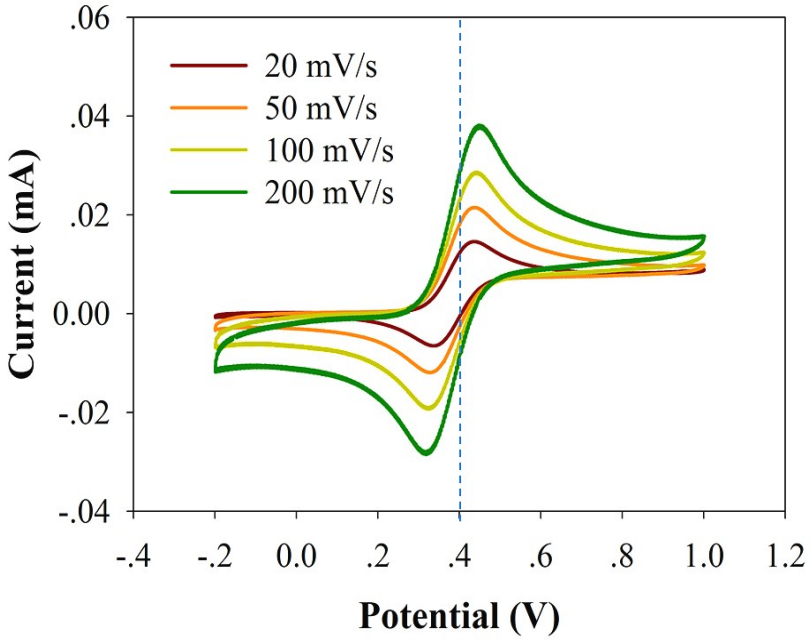

Fig. S10. Cyclic voltammetry (CV) of 1mg/mL ferrocene at scan rates of 20, 50, 100, 200 mV/s. CV was recorded in 5 mL acetonitrile containing 0.1M tetrabutylammonium hexafluorophosphate as the supporting electrolyte with a working gold electrode, a reference silver (Ag/AgCl) electrode and a counter platinum electrode. According to the figure, the formal potential of the Fc^+/Fc redox couple should be approximately 0.40V versus Ag/AgCl.

Cyclic voltammetry (CV) was used to determine the HOMO and LUMO energy levels of the CNDs. A three-electrode cell with a gold working electrode, a silver reference (Ag/AgCl)

electrode and a platinum counter electrode in 4 mL acetonitrile containing 0.1 M tetrabutylammonium hexafluorophosphate as the supporting electrolyte and 1 mL H_2O containing 0.3 mg CNDs as the sample at a scan rate of 100 mV/s under room temperature was used.[5,6] All the potentials were compared with a standard fc^+/fc couple measured in the same solution. Since the potential of SCE is 44 mV more positive than the potential of Ag/AgCl, and the formal potential of the Fc^+/Fc redox couple should be approximately -5.1 eV in the Fermi scale when its value is 0.40 V versus SCE in acetonitrile, the formal potential of the Fc^+/Fc redox couple could be estimated as -5.06 eV in the Fermi scale when the formal potential of the Fc^+/Fc redox is 0.40 V versus Ag/AgCl.

The HOMO and LUMO energy levels as well as the electrochemical energy gap in eV of the sample could be calculated according to the following equation:

$$E_{HOMO}=-(E_{onset,ox}-0.4+5.06)eV=-(E_{onset,ox}+4.66)eV,$$

$$E_{LUMO}=-(E_{onset,red}-0.4+5.06)eV=-(E_{onset,red}+4.66)eV,$$

$$E_{gap}=(E_{onset,ox}-E_{onset,red})eV,$$

where $E_{onset,ox}$ and $E_{onset,red}$ are the onset of oxidation and reduction potential, respectively.

By applying tangent method, on the basis of the onset of oxidation and reduction potential as 1.18 and -0.91 V, the energy levels of the HOMO and LUMO were estimated to be–5.84 and -3.75 eV, respectively. Moreover, the electrochemical band gap was estimated to be 2.09 eV, which is consistent with the optical band gap.

Method 3. Hückel method energy gap calculation

The Hückel method[7] is a linear combination of atomic orbitals molecular orbitals method for the determination of energies of molecular orbitals in conjugated hydrocarbon systems. Then it could be extended to heteroatoms by adjusting the coulomb and resonance integral values. Note that the coulomb integral for an electron on a carbon was defined as α and the resonance integral for two bonded carbons in conjugation was defined as β. In our CQDs system, according to the equations (α'=α+hβ, and β'=kβ) and table S6, α and β were adjusted to α' and β'.[8,9]

Table S6. Adjustment of the coulomb and resonance integral values

Heteroatom	h	Heteroatom Bond	k	Bond Lengths (Å)
C	0	C-C	0.9	1.54
N	1.5	C=C	1.1	1.35
O	2.0	C-O	0.8	1.43
		C=O	1.0	1.22
		C-N	0.8	1.47

Then by solving the following determinant, the Hückel values for our CNDs can be determined following the order of heteroatoms and heteroatom bonds as the assumed molecular structure of CNDs shown (Fig. S11). After that, we can use $E_i = \alpha' + x_i\beta'$ to calculate L+1, L+2, LUMO, HOMO, H-1, and H-2 energy levels. And the magnitudes of the transition moment for different bonds were calculated from a simple model[10] (transition moment equals to half of dipole moment of one charge displaced through the bond length). Note that many computer programs like SHMO or Matlab software can help to solve the determinants.

$$
\begin{vmatrix}
\alpha_1'-E & \beta_{1,2}' & \beta_{1,3}' & \beta_{1,4}' & \cdots\cdots & \beta_{1,n-2}' & \beta_{1,n-1}' & \beta_{1,n}' \\
\beta_{2,1}' & \alpha_2'-E & \beta_{2,3}' & \beta_{2,4}' & \cdots\cdots & \beta_{2,n-2}' & \beta_{2,n-1}' & \beta_{2,n}' \\
\beta_{3,1}' & \beta_{3,2}' & \alpha_3'-E & \beta_{3,4}' & \cdots\cdots & \beta_{3,n-2}' & \beta_{3,n-1}' & \beta_{3,n}' \\
\beta_{4,1}' & \beta_{4,2}' & \beta_{4,3}' & \alpha_4'-E & \cdots\cdots & \beta_{4,n-2}' & \beta_{4,n-1}' & \beta_{4,n}' \\
\cdots\cdots & & & & & & & \\
\beta_{n-2,1}' & \beta_{n-2,2}' & \beta_{n-2,3}' & \beta_{n-2,4}' & \cdots\cdots & \alpha_{n-2}'-E & \beta_{n-2,n-1}' & \beta_{n-2,n}' \\
\beta_{n-1,1}' & \beta_{n-1,2}' & \beta_{n-1,3}' & \beta_{n-1,4}' & \cdots\cdots & \beta_{n-1,n-2}' & \alpha_{n-1}'-E & \beta_{n-1,n}' \\
\beta_{n,1}' & \beta_{n,2}' & \beta_{n,3}' & \beta_{n,4}' & \cdots\cdots & \beta_{n,n-2}' & \beta n,_{n-1}' & \alpha_n'-E
\end{vmatrix} = 0
$$

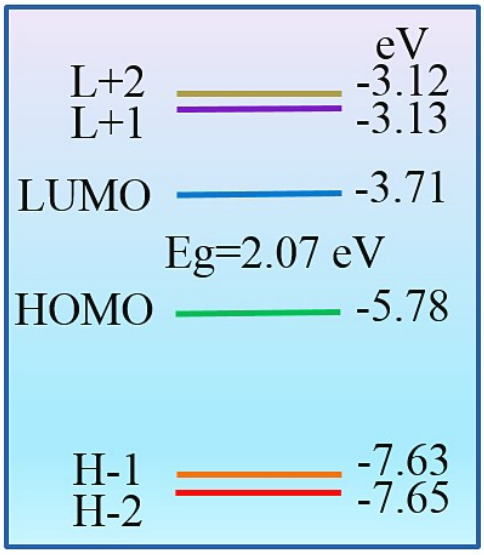

Fig. S11. Molecular orbital energy levels of CNDs calculated by Hückel method.

Table S7. Transition moments for different bonds

Bond	Bond Lengths (Å)	Transition Moment (D)
C=C	1.35	3.24
C=O	1.22	2.93
C-O	1.43	3.43
O-H	0.96	2.30

Reference

1. Melhuish, W. H. (1961). Quantum efficiencies of fluorescence of organic substances: effect of solvent and concentration of the fluorescent solute1. *The Journal of Physical Chemistry*, *65*(2), 229-235.

2. Yu, D., Yang, Y., Durstock, M., Baek, J. B., & Dai, L. (2010). Soluble P3HT-grafted graphene for efficient bilayer− heterojunction photovoltaic devices. *ACS nano*, *4*(10), 5633-5640.

3. Harb, M. (2015). Predicting suitable optoelectronic properties of monoclinic VON semiconductor crystals for photovoltaics using accurate first-principles computations. *Physical Chemistry Chemical Physics*, *17*(38), 25244-25249.

4. Moses, D., Wang, J., Heeger, A. J., Kirova, N., & Brazovski, S. (2001). Singlet exciton binding energy in poly (phenylene vinylene). *Proceedings of the National Academy of Sciences*, *98*(24), 13496-13500.

5. Cardona, C. M., Li, W., Kaifer, A. E., Stockdale, D., & Bazan, G. C. (2011). Electrochemical considerations for determining absolute frontier orbital energy levels of conjugated polymers for solar cell applications. *Advanced materials*, *23*(20), 2367-2371.

6. Zou, Y., Najari, A., Berrouard, P., Beaupré, S., Réda Aïch, B., Tao, Y., & Leclerc, M. (2010). A thieno [3, 4-c] pyrrole-4, 6-dione-based copolymer for efficient solar cells. *Journal of the American Chemical Society*, *132*(15), 5330-5331.

7. Liu, Y., Jiang, S., Glusac, K., Powell, D. H., Anderson, D. F., & Schanze, K. S. (2002). Photophysics of monodisperse platinum-acetylide oligomers: Delocalization in the singlet and triplet excited states. *Journal of the American Chemical Society*, *124*(42), 12412-12413.

8. http://www.utdallas.edu/~biewerm/5-applications.pdf

9. http://iqscience.richmond.edu/course/materials/Geometries.pdf

10. http://www4.ncsu.edu/~franzen/public_html/CH736/lecture/Intro_to_Molecular_Spectra.pdf